

Investigations on the gas-phase photolysis and OH radical kinetics of nitrocatechols: Implications of intramolecular interactions on their atmospheric behavior

Claudiu Roman^{1,2}, Cecilia Arsene^{1,2}, Iustinian Gabriel Bejan^{1,2}, Romeo Iulian Olariu^{1,2*}

5 ¹“Alexandru Ioan Cuza” University of Iasi, Faculty of Chemistry, Iasi, 11th Carol I, 700506, Romania

²“Alexandru Ioan Cuza” University of Iasi, Integrated Center of Environmental Science Studies in the North Eastern Region - CERNESIM, Iasi, 11th Carol I, 700506, Romania

*Correspondence to: Olariu Romeo Iulian (oromeo@uaic.ro)

Abstract. The Environmental Simulation Chamber made of Quartz from the University “Alexandru Ioan Cuza” from Iasi (ESC-Q-UAIC), Romania, was used to investigate for the first time the gas-phase reaction rate coefficients for four nitrocatechols towards OH radicals under simulated atmospheric conditions. Employing relative rate techniques at a temperature of 298 ± 2 K and total air pressure of 1 atm, the obtained rate coefficients (in $10^{-12} \text{ cm}^3 \cdot \text{s}^{-1}$) were as follows: $k_{3\text{NCAT}} = (3.41 \pm 0.37)$ for 3-nitrocatechol, $k_{4\text{NCAT}} = (1.27 \pm 0.19)$ for 4-nitrocatechol, $k_{5\text{M3NCAT}} = (5.55 \pm 0.45)$ for 5-methyl-3-nitrocatechol and $k_{4\text{M5NCAT}} = (0.92 \pm 0.14)$ for 4-methyl-5-nitrocatechol. For the investigated compounds the photolysis rates in the actinic region, scaled to atmospheric relevant conditions by NO_2 photolysis, were evaluated for 3-nitrocatechol and 5-methyl-3-nitrocatechol: $J_{3\text{NCAT}} = (3.06 \pm 0.16) \times 10^{-4} \text{ s}^{-1}$ and $J_{5\text{M3NCAT}} = (2.14 \pm 0.18) \times 10^{-4} \text{ s}^{-1}$, respectively. Considering the obtained results, our study suggests that photolysis may be the main degradation process for 3-nitrocatechol and 5-methyl-3-nitrocatechol in the atmosphere, with a photolytic lifetime in the atmosphere up to 2 hours. Results are discussed in terms of the reactivity of the investigated four nitrocatechols towards OH-radical initiated oxidation and their structural features. The rate coefficient values are also compared with those estimated from the structure-activity relationship for monocyclic aromatic hydrocarbons and discussed with gas-phase IR spectra of the nitrocatechols. Additional comparison with similar compounds is also presented underlining the implications towards possible degradation pathways and atmospheric behavior.

1. Introduction

Aromatic hydrocarbons (AHs) are a class of volatile organic compounds (VOCs) present as primary pollutants in the atmosphere mainly because of the anthropogenic activities. In urban areas, AHs are present due to the use of solvents, incomplete combustion of fossil fuels, car-engine emissions and industrial processes (Piccot et al., 1992). Various monocyclic aromatics occur from biomass burning in rural and remote areas (Schauer et al., 2001). Atmospheric removal of these compounds occurs via reactions with different oxidants (Finlayson-Pitts and Pitts, 2000) and by wet and dry deposition (Calvert et al., 2002; Warneck, 2000). The gas-phase oxidation initiated by the OH radicals is the main reaction responsible

30 for the atmospheric sink of aromatic hydrocarbons. The chemical degradation of AHs forms oxidation products which further could be aromatic in nature or could lead to open ring compounds. AHs are known also as important contributors to the photo-oxidants and secondary organic aerosols (SOA) formation in the atmosphere (Calvert et al., 2002; Jenkin et al., 2017).

Hydroxylated aromatic compounds, such as phenol (Atkinson et al., 1992; Berndt and Böge, 2003; Sørensen et al., 2002),
35 cresols (Atkinson et al., 1992; Coeur-Tourneur et al., 2006), dimethyl-phenols (Thüner et al., 2004), trimethyl-phenols (Bejan et al., 2012), methoxy-phenols, (Lauraguais et al., 2015) and catechols (Olariu et al., 2000) are the most reactive species towards OH radicals. According to Master Chemical Mechanism (MCM), version 3.3.1 (Bloss et al., 2005), which describes the detailed gas-phase chemical processes involved in the tropospheric degradation of a series of primary emitted VOCs, the major oxidation pathway for monocyclic aromatic compounds is the addition of the OH radical to the aromatic 40 ring that may lead to the ring retaining products. The distribution of the hydroxylated isomers varies for each monocyclic aromatic compound depending on the stability of its OH-adduct. Thus, the OH-addition reactivity channel will lead to the formation of phenol and cresols with a range of yields from 5 to 50% in the case of benzene and toluene. These formation yields are very much affected by the levels of NO_x (NO_x = NO + NO₂) in the reaction mixture, and the formation yields of the mono-hydroxylated aromatic compounds is decreasing in the presence of high NO_x concentration (Atkinson and 45 Aschmann, 1994; Klotz et al., 1998, 2002; Volkamer et al., 2002). The hydroxylated products, when photo-oxidized by the OH radicals under atmospheric conditions, in turn form catechols with formation yields of about 65 to 90% (Olariu et al. 2002). Formation of nitrophenols and nitrocatechols from the oxidation of phenols and catechols initiated by the OH radicals is assigned to the H-atom abstraction pathway from the phenolic hydroxyl group, accounting for about 10% in the mono-hydroxylated aromatic compounds and for about 30% in the di-hydroxylated aromatic compounds (Atkinson et al., 1992; 50 Finewax et al., 2018; Olariu et al., 2002). High formation yields of nitrophenols (more than 50%) and nitrocatechols (close to 100%) were reported from the gas-phase reactions of the NO₃ radical with the phenols and catechols, which may support the fact that the NO₃ chemistry may have an important role in the formation of such nitroaromatic compounds (Finewax et al., 2018; Olariu et al., 2004, 2013).

Nitroaromatic hydrocarbon compounds (NAHs) have been found in particulate matter (Delhomme et al., 2010; Herterich and 55 Herrmann, 1990), rainwater (Belloli et al., 2006; Grosjean, 1991), clouds (Lüttke et al., 1997), water (Herterich, 1991; Rubio et al., 2012), snow (Leuenberger et al., 1988), soil (Vozňáková et al., 1996) and fog (Harrison et al., 2005; Richartz et al., 1990) and even in remote areas as in Terra Nova Bay, Antarctica (Vanni et al., 2001). More recently, nitroaromatics have been reported in aerosol composition (Vidović et al., 2018) from urban area sampled from Nagoya-Japan (Ikemori et al., 2019), Paris-France (Lanzafame et al., 2021), Beijing-China (Wang et al., 2021). Nitrocatechols have been found as tracer 60 compounds in particulate matter emitted during biomass burning, correlating well with the levoglucosan and NO_x levels (Kitanovski et al., 2012b, 2012a; Salvador et al., 2021). In organic aerosols the 4-nitrocatechol concentration exceeds in some cases 150 ng × m⁻³ while for methylated nitrocatechols the overall concentration can be as high as 821 ng × m⁻³ (Inuma et al., 2010; Kitanovski et al., 2020). These high concentrations of nitrated monoaromatic hydrocarbons were

determined in the winter season and have been correlated with household wood burning use. However, in these studies, all 65 identified nitrocatechols seem to cover up to 96% of the nitrated monoaromatic hydrocarbons found in PM10 samples (Kitanovski et al., 2020). 4-nitrocatechol was found in the reaction of guaiacol initiated by OH radicals in the presence of NO_x (Lauraguais et al., 2014). Besides 4-nitro-, 3-nitro- and 6-nitroguaiacol formed as oxidation products, occurrence of 4-nitrocatechol was explained via the *-ipso* addition channel of OH radical to the methoxy group. Schwantes et al. (2017) report the formation of highly oxygenated low-volatile products from the chamber studies of *o*-cresol oxidation under high 70 NO_x conditions. The signal with m/z = 169 detected by mass spectrometric techniques has been attributed to methyl-dihydroxy-nitrobenzene. Finewax et al. (2018) have reported 4-nitrocatechol in secondary organic aerosol (SOA) composition from the gas-phase oxidation of catechol initiated by both OH (30%) and NO₃ (91%) radicals, respectively. Atmospheric production of nitroaromatic compounds, including nitrophenols, dinitrophenols and nitrocatechols, is of great 75 interest as they play a significant role in the formation of brown carbon and aerosols (Lin et al., 2016). Their low atmospheric reactivity and high ability to absorb large amounts of near-UV, visible and infrared radiation could lead to positive radiative forcing (Bejan et al., 2007; Zhang et al., 2017).

The present study aims to determine and discuss, for the first time upon our knowledge, the OH kinetic rate coefficients for 80 four nitrocatechols: 3-nitrocatechol (3NCAT), 4-nitrocatechol (4-NCAT), 5-methyl-3-nitrocatechol (5M3NCAT) and 4-methyl-5-nitrocatechol (4M5NCAT) by using the Environmental Simulation Chamber made of Quartz from University “Alexandru Ioan Cuza” from Iasi, Romania (ESC-Q-UAIC). Based on the ESC-Q-UAIC facilities, the photolysis frequencies of the investigated compounds were evaluated and scaled to the relevant atmospheric conditions. Detailed 85 investigations with impact on the reactivity of highly substituted nitro-aromatic compounds are also depicted in this work.

2. Experimental

Gas phase rate coefficients of the studied nitrocatechols towards OH radicals have been determined using the relative kinetic 85 method. For this purpose, the ESC-Q-UAIC reactor, a 760 L and 4.2 m long cylindrical photoreactor consisting of three quartz tubes surrounded by 32 Philips TL-DK 36W (with $\lambda_{\text{max}}=365$ nm) and 32 UV-C TUV 30W/G30 T8 (with $\lambda_{\text{max}}=254$ nm), has been employed. Experiments were performed at 1 atm of air and temperature of 298 ± 2 K. Decay of the 90 nitrocatechols and reference compounds in the reactor vessel was monitored by IR spectroscopy using a Bruker Vertex 80 FTIR coupled to a White type mirrors system mounted inside the chamber, providing a total optical path of 492 ± 1 m. Solid nitrocatechols were transferred into the reactor at low pressure, via a preheated glassware port. A steam of nitrogen flowing 95 over the heated nitroaromatic compound was used to carry the reactants and reference compounds inside the reaction chamber. Two Teflon blade fans were used to ensure homogeneous mixture. Dimethyl ether (C₂H₆O), cyclohexane (C₆H₁₂) and methanol (CH₃OH) were chosen as reference compounds in the relative kinetic study due to their IR spectral features and well-known rate coefficients for the reaction with OH radicals, rate coefficients close to those of the investigated compounds: $k_{\text{C}_2\text{H}_6\text{O}} = (2.80 \pm 0.56) \times 10^{-12} \text{ cm}^3 \times \text{s}^{-1}$ (Atkinson et al., 2004), $k_{\text{C}_6\text{H}_{12}} = (6.38 \pm 0.56) \times 10^{-12} \text{ cm}^3 \times \text{s}^{-1}$ (Wilson et

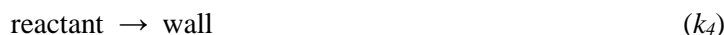
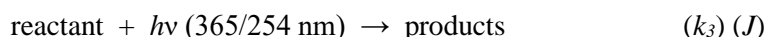
al., 2006) and $k_{\text{CH}_3\text{OH}} = (0.90 \pm 0.18) \times 10^{-12} \text{ cm}^3 \times \text{s}^{-1}$ (Atkinson et al., 2004). Dimethyl ether (DME) was used as reference hydrocarbon for all the investigated nitrocatechols while cyclohexane was used for the kinetic studies involving 3-nitrocatechol and 5-methyl-3-nitrocatechol. Methanol was employed for the kinetic experiments of 4-nitrocatechol and 4-methyl-5-nitrocatechol. The OH radicals were generated *in situ*: (1) via photolysis of a mixture of $\text{CH}_3\text{ONO}/\text{NO}$ at 365 nm as shown in R1.1 to R1.4 reactions, where NO has been added in excess to suppress ozone formation and potential interference processes in the reaction kinetics:



and (2) via photolysis of H_2O_2 at 254 nm for 4-nitrocatechol and 4-methyl-5-nitrocatechol as presented in R2.1 reaction



Preliminary tests showed that nitrocatechols photo-dissociate under experimental conditions. Corrections to reactants' concentration are needed to be made due to the photolysis and wall deposition, as presented in the following reactions sequence:



115 By representing the total decay of both reference and reactant in time, with respect to the correction mentioned above, the following kinetic expression shown in Eq. 1 could be used to determine the nitroaromatic rate coefficients:

$$\ln \frac{[\text{reactant}]_{t_0}}{[\text{reactant}]_t} - (k_3 + k_4)(t - t_0) = \frac{k_1}{k_2} \ln \frac{[\text{reference}]_{t_0}}{[\text{reference}]_t} \quad (\text{Eq. 1})$$

where $[\text{reactant}]_{t_0}$ and $[\text{reference}]_{t_0}$ are the initial concentrations of nitrocatechols and the reference compound at t_0 , and

120 $[\text{reactant}]_t$ and $[\text{reference}]_t$ are the concentrations of nitrocatechols and the reference compounds during the reaction time t , k_1 , k_2 are the gas phase rate coefficients for the OH radical reactions with the reactants and reference compounds respectively, k_3 is the photolysis frequency (J) of the reactants at 365/254 nm and k_4 is the wall loss rate coefficient. The ratio of k_1/k_2 determined from the slope of the linear regression is used further to obtain the rate coefficient k_1 by using well determined k_2 rate coefficients of the reference compounds. No wall loss or photolysis was observed for the reference hydrocarbons used in this study.

However, the photolysis of nitrocatechols at 254 and 365 nm has been measured using CO as OH-radical scavenger. Photolysis rate coefficients are corrected for wall loss and used to correct further rate coefficients from the reactions of nitrocatechols with OH radicals.

Initial concentrations of reactants in the reactor were: $6.5 \times 10^{13} \text{ cm}^{-3}$ for DME, $4.8 \times 10^{13} \text{ cm}^{-3}$ for cyclohexane, $12.5 \times 10^{13} \text{ cm}^{-3}$ for methanol, $12.9 \times 10^{13} \text{ cm}^{-3}$ for NO, $16.2 \times 10^{13} \text{ cm}^{-3}$ for CH_3ONO , a maximum of $25.2 \times 10^{13} \text{ cm}^{-3}$ for H_2O_2 . For the investigated nitrocatechols their initial concentration varied between $(2.5 - 7.7) \times 10^{13} \text{ cm}^{-3}$.

3. Chemicals

Chemical compounds used in the present study were: DME >99.9% (suitable for GC analysis, Sigma-Aldrich), cyclohexane >99.5% (anhydrous, Sigma-Aldrich), methanol (anhydrous, >99.9% suitable for HPLC analysis, Sigma-Aldrich), NO 135 >99.5% purity, Linde), H_2O_2 (40% solution in water, Sigma-Aldrich), CO (>99.997% purity, Linde). CH_3ONO was prepared in our laboratory using an adapted method from [Taylor et al. \(1980\)](#). All nitrocatechols have been synthesized using two methods of nitration according to available literature information proposed by [Rosenblatt et al. \(1953\)](#) and adapted by [Iinuma et al. \(2010\)](#) and [Palumbo et al. \(2002\)](#). Thus, both 3-nitrocatechols have been obtained by treating an anhydrous 140 diethyl ether solution of the corresponding catechols with freshly prepared fuming nitric acid. 4-nitrocatechol and 4-methyl-5-nitrocatechols were prepared by treating a cooled aqueous solution of catechol and sodium nitrite with sulfuric acid. Extractions and purifications of the synthesized compounds were conducted by means of sublimation and recrystallization. The purity of the synthesized compounds from H-NMR analysis was found to be about 98% ([Roman et al., 2022](#)).

4. Results

Kinetic results for the reaction of nitrocatechols with OH radicals are presented in Figures 1 to 4. For each compound, a 145 minimum of four experiments have been performed. Despite difficulties in handling these low volatile compounds, their slow reactivity towards OH radicals, and the difficulties encountered in the IR spectra evaluation, the plots depicted in Figures 1 to 4 show good linearity. Total conversion of nitrocatechols during the irradiation period was evaluated to range from about 25% to 55 %. Up to 60% of the decays of the nitrocatechols and the reference compounds have been attributed to the reaction with OH radicals during the kinetic experiments.

150 Table 1 presents the kinetic data results from the present study. Relative ratios of k_1/k_2 determined from the kinetic plots (see Figures 1 to 4), gas-phase rate coefficient (k_1) calculated for the OH reactions with the investigated nitrocatechols, and the average kinetic coefficients ($k_1\text{average}$) are also indicated in Table 1. Uncertainties for the k_1/k_2 represent 2σ from the linear regression analysis. The k_1 rate coefficient errors are given from a combination of 2σ values from the linear regression and an additional error from the reference compound uncertainty. As for the k_1 (average) and its uncertainty, the weighted 155 average was used to estimate the best interval that accommodates the highest confidence of the obtained data. Based on the

daytime average concentration of the OH radicals in the atmosphere (Prinn et al., 1995), of $1.6 \times 10^6 \text{ cm}^{-3}$, Table 1 lists also the atmospheric residence time of the studied nitrocatechols. No significant differences were observed for 4-nitrocatechol and 4-methyl-5-nitrocatechol rate coefficient values when NO_x or NO_x-free conditions have been employed.

Direct photolysis of the hydroxylated nitroaromatics under similar conditions as those used in this study have been shown to 160 produce HONO (Bejan et al., 2006), similar to the carboxylic acid formation mechanism in aqueous phase proposed by Alif et al. (1991). Photolysis of HONO is a well-known source of OH radicals. To properly evaluate the photolysis rate coefficients at 365 nm and 254 nm for the investigated nitrocatechols by accounting for possible interference of the secondary chemistry due to the OH radicals' reactions, a series of individual experiments were performed using carbon monoxide (CO) as OH scavenger. To override the low reactivity of the scavenger ($k_{\text{CO+OH}} = 2.41 \times 10^{-13} \text{ cm}^3 \times \text{s}^{-1}$) (DeMore et 165 al., 1994), a high amount of CO was introduced into the reactor vessel (of about $1.17 \times 10^{17} \text{ cm}^{-3}$) to ensure a scavenging efficiency of more than 98%. Photolysis rates for all four nitrocatechols at 365 nm (J_{365}) were evaluated. At this wavelength, no significant photolysis for 4-nitrocatechol and 4-methyl-5-nitrocatechol was observed, while for 3-nitrocatechol and 5-methyl-3-nitrocatechol photolysis frequencies of $(1.53 \pm 0.08) \times 10^{-4} \text{ s}^{-1}$ and $(1.07 \pm 0.09) \times 10^{-4} \text{ s}^{-1}$, respectively, have been measured (see Figure S1 from Supplementary Material - SM). Additionally, since for 4-nitrocatechol and 4-methyl-5- 170 nitrocatechol the reaction rate coefficients were measured under NO_x free condition by using H₂O₂ photolysis as OH radical precursor, photolysis rate coefficients at 254 nm of these two compounds were evaluated. For 4-nitrocatechol the photolysis rate (J_{254}) was $(6.71 \pm 0.99) \times 10^{-5} \text{ s}^{-1}$ and that for 4-methyl-5-nitrocatechol was $(3.18 \pm 0.32) \times 10^{-5} \text{ s}^{-1}$ (see Figure S2 from SM). However, for 3-nitrocatechol and 5-methyl-3-nitrocatechol corrections have been also performed because of their high 175 wall loss and their photolysis at 365 nm. Photolysis rate coefficients are presented in Table 2, beside the average lifetime with respect to photolysis under atmospheric conditions. Photolysis rate coefficients at 365 nm for 3-nitrophenols has been scaled to the atmospheric conditions, as Klotz et al. (1997) have described for 40° N latitude noontime and clear sky conditions, with a factor of 2 obtained from the NO₂ photolysis frequency measured in atmospheric conditions versus the ESC-Q-UAIC reactor ($J_{\text{NO}_2 - \text{atmosphere}} / J_{\text{NO}_2 - \text{ESC-Q-UAIC chamber}} = 8.5 \times 10^{-3} \text{ s}^{-1} / 4.3 \times 10^{-3} \text{ s}^{-1} \approx 2$). The wall loss (k_4) measured for 3NCAT and 5M3NCAT was about $(3.2 \pm 0.4) \times 10^{-4} \text{ s}^{-1}$, while for 4NCAT and 4M5NCAT of about $(0.7 \pm 0.3) \times 10^{-4} \text{ s}^{-1}$. 180 However, the wall loss was relatively constant over different experiments employed in this study. Average quantum yields calculated for 3NCAT and 5M3NCAT over the 350-400 nm range were obtained using the theoretical approach described by Hofzumahaus et al. (1999), and the evaluated cross-sections of these two compounds in aqueous solutions are presented in Table TS1 in the Supplementary Material (SM). The average quantum yields, calculated for the investigated range ($\phi_{350-400}$), are: $(7.707 \pm 0.737) \times 10^{-3}$ for 3NCAT and $(4.858 \pm 0.464) \times 10^{-3}$ for 5M3NCAT. The overall errors include contributions 185 from the solution preparation, UV-VIS spectra recording (see Figure S3 from SM) and the photolysis values. A detailed description of the technique, data collection, evaluation and interpretation is presented in the SM. However, preliminary analysis of the residual spectra obtained after irradiation of 3NCAT and 5M3NCAT, presented in Figure S4 in the SM, reveals one signal that could be representative for a ketene-type product.

The rate coefficients obtained from the kinetic investigations of a series of nitrocatechols with OH radicals are reported for the first time in this study. No significant differences have been observed between the two reference compounds that have been employed to achieve the quality of the rate coefficient values. Based on collision theory and the standard gas kinetic theory, [Sørensen et al. \(2002\)](#) showed that the presence of inorganic aerosols does not influence the value of the OH radicals rate coefficients when relative kinetic technique is used. Deactivation rate of the OH radicals due to the presence of aerosols in the reaction chamber was estimated by considering an OH radicals average velocity of about $6.09 \times 10^4 \text{ cm} \times \text{s}^{-1}$ at 298 K ([Atkins and de Paula, 2006](#)) and the experimental conditions employed in this study, relative to the particles area per air unit volume initially formed into the system ([Roman et al., 2022](#)). Under these conditions, the contribution of the deactivation process is less than 1% for 3-nitrocatechol and 5-methyl-3-nitrocatechols and between 7-21% for 4-nitrocatechol and 4-methyl-5-nitrocatechol. However, even if such process occurs at higher rate, using of the relative kinetic technique, where the k_1/k_2 ratio is experimentally determined independent of the OH radical concentration of, no systematic errors rising up from the OH radical concentration would influence the kinetic data. On the other hand, possible SOA formation from the irradiation of nitrocatechols is expected following a similar process as the one reported by [Bejan et al. \(2020\)](#) for nitrophenols. However, these would also not influence the kinetic data even if expected effects on the gas phase nitrocatechols concentration due to the gas-particle equilibrium are not excluded. Taken into account estimations for Henry's law constant of $(2 - 8) \times 10^{-13} \text{ atm} \times \text{m}^3 \times \text{mole}^{-1}$ at 25°C, this effect is unlikely to make significant differences over the nitrocatechols concentrations used in the present study ([Hine and Mookerjee, 1975](#); [Meylan and Howard, 1991](#)). A comparison with literature data is not possible. However, there are reported rate coefficient values for nitrophenol and methylated nitrophenols reaction with OH radicals ([Atkinson et al., 1992](#); [Bejan et al., 2007](#)). Additionally, kinetic rate coefficients of the OH radical initiated oxidation of nitronaphthalene have been studied by [Atkinson et al. \(1989\)](#). For the OH radical reactions with the nitroaromatic compounds, however, all the reported values of the rate coefficients in the literature have the same order of magnitude of $10^{-12} \text{ cm}^3 \times \text{s}^{-1}$, as those presented in this work.

5.1. Electromeric effect of aromatic ring substituents

Prior to initiate the discussions on the kinetic results, we should emphasize the influence of the substituent position on the 215 aromatic ring for all the nitrocatechols and their effect on the reactivity. The electromeric effects influencing reactivity could be easily noticed on the structure of infrared spectra. Figure 5A presents the gas-phase infrared spectra of catechol (CAT), 3NCAT and 4NCAT and Figure 5B the gas-phase infrared spectra of 4-methylcatechol (4MCAT), 5M3NCAT and 4M5NCAT. Infrared spectra clearly show the presence of the H-bonds between OH (vibrations being marked with * and **) and NO₂ groups substituents attached to the aromatic ring in the nitrocatechols as follows: the compounds 3NCAT and 220 5M3NCAT exhibit a H-bond between the OH and one of the O atom from the NO₂ vicinal group; 4NCAT presents a H-bond between the H from the C1-linked OH and the O atom from the C2-linked OH; and 4M5NCAT reveal a H-bond bond

between the H from the C2-linked OH and the O atom from the C1-linked OH in 4M5NCAT similar to 4NCAT. One could notice the existence of similar structure of vicinal OH groups in catechol and 4-methylcatechol. However, these H-bonds are not present in CAT and 4MCAT, as both OH groups are highlighted in the gas phase IR spectra. H- bond occurring in the 225 nitrocatechols should be evaluated in the light of the existent nitro group that acts with its deactivating electromeric E- effect on the ring, withdrawing the electrons from its *-ortho* and *-para* positions. For the 3-nitrocatechols, the chemical structures reveal the presence of one OH group placed between the OH and NO₂ groups. This hydroxyl group will be affected by the 230 electron withdrawing effect of NO₂, and in consequence, the weakened O-H bond results in an H-atom that is more susceptible to form a H-bond with the O from the NO₂ group. This bond can be observed also in the IR spectra of 2-nitrophenols (Figure S5 from the SM) (Bejan et al., 2007; Bejan, 2006; Olariu et al., 2002, 2013) and is considered to be 235 responsible for SOA and HONO formation via H-atom transfer during gas-phase photolytic processes (Bejan et al., 2006, 2020). As shown in the spectra from Figure 5A and Figure 5B, the structure of CAT and 4MCAT exhibit the presence of OH groups one next to the other and no visible H-bond between these substituents. These suggest that for 1,2-dihydroxybenzenes the E+ effect is less diminished through the presence of the vicinal OH in *-ortho* to the first one.

235 In Figure 6, 3NCAT has been chosen as a master example to emphasize the electromeric effects manifested by NO₂ and OH groups on the aromatic ring, in order to identify also their possible implications on the molecule stability. For the 3NCAT structure, one could observe that the OH substituent next to NO₂ group would produce an H bond which is shielded to manifest its E+ effect on the ring. As reported by Bejan et al. (2006, 2020), photolysis of methylated 2-nitrophenols leads to 240 HONO formation via H-transfer from the hydroxyl group its vicinal nitro group. For 4NCAT and 4M5NCAT, where both OH are linked in the H-bonds, no significant photolysis at 365 nm and no E+ effect to enhance electron density on the aromatic ring occur.

5.2. Reactivity trends

It is well known that the presence of a nitro group has a high deactivating effect on the aromatic ring as the reactivity of 245 nitroaromatic compounds are approximatively 5-20 time lower than their parent compounds. Some OH rate coefficients at 298 K for AHs and their corresponding NAHs are presented in Table 3. The reactivity of catechols against OH radicals drops even more than two order of magnitude when a nitro group is attached to the ring (Olariu et al., 2000). Such a sudden loss in reactivity is due to the inhibition of the addition channel in aromatic hydrocarbons as discussed in the present study. Ring 250 retaining product studies from the gas phase OH-radical initiated oxidation of phenol and cresols show that the addition pathway is the dominant oxidation mechanism, occurring between 65% up to 90% of the overall reactions, nitrophenols being formed via phenolic H-atom abstraction channel accounting for 5% to 10 % (Olariu et al., 2002). Gas-phase reactions with NO₃ radicals lead to a yield of ~50% of nitrocatechols and almost 100% of nitric acid suggesting that the H-atom abstraction channel represents at least half of the overall reactions (Olariu et al., 2013). In the gas-phase oxidation of catechol with OH radical at high NO_x conditions, Finewax et al. (2018) found 4NCAT in the SOA composition with a molar yield of 30%. At least 90% molar yield has been obtained in their study in the oxidation initiated by NO₃ radicals. These

255 results suggest that H-atom abstraction channel has a greater contribution in catechols reactivity rather than abstraction channel from phenol or cresols oxidation.

The gas phase rate coefficients in the investigated series of nitrocatechols vary as follow: $k_{5M3NCAT} > k_{3NCAT} > k_{4NCAT} \sim k_{4M5NCAT}$. 4NCAT and 4M5NCAT could assume a little effect from the methyl group but little distinguished from experimental determined rate coefficients values from this study. A distribution of possible free attack sites by OH radicals 260 on the aromatic ring, accounted also by the substituent's effects, is represented in Figure 7 A. The NO_2 group deactivates the aromatic ring towards OH attack by the E- effect. By its I+ effect, the $-\text{CH}_3$ substituent will probably influence the electrophilic addition, although its effect is diminished by the E- from the $-\text{NO}_2$ substituent. According to Figure 7 A, the most stable adduct is the 4M5NCAT-OH, and one could propose an OH radical addition to the 3rd position of the ring. 265 However, this is not the case since the experimental data shows that 4M5NCAT is the least reactive compound in this series, because of the substituent's interactions (see Figure 7 B). Differences between the reactivity of 3NCAT and 5M3NCAT in reaction with an electrophile suggest two determining pathways to occur: addition to the ring in the NO_2 -deactivated 4th or 270 6th position oriented by the E+ electromeric effect of OH (C1) and I+ effect from CH_3 , and H-atom abstraction from the C1 linked OH group. While the difference between 3NCAT and 5M3NCAT is comparable with the difference between 2-nitrophenol (2NPh) and 4-methyl-2-nitrophenol (4M2NPh), we may consider that the E+ effect of OH (C1) is less present 275 due to the same orientation of the E- effect of NO_2 . Comparing the reactivity of 2NPh with those of methyl-2-nitrophenols, an increase in the reactivity of 2 up to 7 times is observed which is attributed to CH_3 group presence and orientation. The most reactive compound is 5-methyl-2-nitrophenol (5M2NPh) with a $k_{5M2NPh} = 6.72 \times 10^{-12} \text{ cm}^3 \times \text{s}^{-1}$, where the methyl I+ effect is manifested on both *-ortho* positions relative to itself and is not affected by the NO_2 E- deactivating effect. In comparison, 4M2NPh, $k_{4M2NPh} = 3.59 \times 10^{-12} \text{ cm}^3 \times \text{s}^{-1}$, both *-ortho* positions to methyl are likely deactivated by the NO_2 . In 280 the methylated nitrophenol series, [Bejan et al. \(2007\)](#) found that the least reactive is 6-methyl-2-nitrophenol (6M2NPh), $k_{6M2NPh} = 2.70 \times 10^{-12} \text{ cm}^3 \times \text{s}^{-1}$, with just one *-ortho* and one *-para* position that are both deactivated by NO_2 . Following the trend for 3-nitrocatechols with respect to the internal electromeric effects of the OH and NO_2 groups and considering the reactivity trend in methyl-2-nitrophenols ([Bejan et al., 2007](#)) and the implication of the methyl group ([Aschmann et al., 2013; Bejan et al., 2012; Klotz et al., 1998](#)) on the addition of OH radical to the (hydroxylated) aromatic hydrocarbons 285 ([Olariu et al., 2000](#)), the rate coefficient for 6M3NCAT (not measured in this study) was estimated to fall between (5.0 - 6.5) $\times 10^{-12} \text{ cm}^3 \times \text{s}^{-1}$, similar to 5M3NCAT.

For 4NCAT and 4M5NCAT, the difference in the reactivity is not obvious since both OH groups involved in H-bond have their E+ effect shielded by the H-bond. If OH group could manifest its electromeric effect, the most reactive compound should be 4M5NCAT. However, the supplementary I+ effect of methyl group, *-para* orientated from the C1-linked OH in 4M5NCAT, seems to strengthen the C1 O-H bond making harder the H abstraction. Even if H-abstraction from CH_3 could be an option for 4M5NCAT, the overall reactivity of this compound is smaller or at least the same as 4NCAT, H-abstraction from the OH group C1-linked being the main degradation path. Seeking the trend in 4-nitrocatechols and 5-nitrocatechols based on these experimental observations, we could estimate that for 3M4NCAT the OH rate coefficient falls in between

(0.5 - 0.9) $\times 10^{-12}$ cm³ \times s⁻¹ and for 3M5NCAT in between (1.0 - 1.4) $\times 10^{-12}$ cm³ \times s⁻¹. However, for all 4-nitrocatechols and 5-nitrocatechols, the rate coefficients could be considered around 1×10^{-12} cm³ \times s⁻¹. These estimations should be treated carefully, since few experimental data are available at this time.

5.3. Comparison with SAR estimated values

There are two Structure-Activity-Relationship (SAR) models for estimating kinetic rate coefficients of aromatic hydrocarbons, both based on substituent factor analysis that influence the reactivity at atmospheric relevant conditions. The general model proposed by [Kwok and Atkinson \(1995\)](#) (used mainly for aliphatic hydrocarbons) considers four cumulative reactions pathways for the OH-initiated oxidations: H-atom abstraction from ring substituents, OH radical addition to the unsaturated aliphatic (double or triple) bond of the substituents, OH radical addition to the aromatic ring and OH radical interactions with ring heteroatoms. The rate coefficient for the total reaction is assumed as a sum of rate coefficients from these four pathways. As for aromatics, this model proposes standard values for H-atom abstraction for the group rate coefficients and substituents factors. For addition to the aromatic ring, the Hammett constants for electrophilic addition, σ^+ , given by [Brown and Okamoto \(1958\)](#) have been proposed by [Zetzs \(1982\)](#) and updated by [Kwok and Atkinson \(1995\)](#) to fit to the equation $\log(k_{\text{add}} / \text{cm}^3 \times \text{s}^{-1}) = -11.71 - 1.34 \times \sum \sigma_i^+$, where the most negative value of the sum $\sum \sigma_i^+$ has to be considered alone and any interaction among the substituents is neglected. The SAR estimation model from [Jenkin et al. \(2018a, 2018b\)](#) updates the factors used in the calculation of rate coefficients and branching ratios for the gas-phase reactions of the OH radicals with monocyclic aromatic compounds. A scaling parameter for the OH radical addition to each carbon atom in the aromatic cycle relative to positions of the ring substituents was introduced. Additionally, for the addition pathway, 17 possible ring substituents adjustment factors were introduced, including nitro and hydroxyl groups. In the H-atom abstraction pathway from aliphatic substituents, another scaling factor for group rate coefficients of $\exp(140/T)$ is recommended to be used when alkyl substituents are present in *-ortho* or *-para* position relative to the attack site. Based on previous gas-phase kinetic and products studies on OH-radical initiated oxidation of hydroxylated aromatic compounds, employed for cresols ([Coeur-Tourneur et al., 2006](#); [Olariu et al., 2002](#)), methoxyphenols ([Coeur-Tourneur et al., 2010b, 2010a](#)), catechols ([Finewax et al., 2018](#); [Olariu et al., 2000](#)) and nitrophenols ([Bejan et al., 2007, 2020](#)), an abstraction rate coefficient from the phenolic OH of $k_{\text{abs}}(\text{Ph-OH}) = 2.6 \times 10^{-12}$ cm³ \times s⁻¹ is being proposed by [Jenkin et al. \(2018b\)](#), a rate coefficient that is 20 times larger than those observed in aliphatic alcohols ([Jenkin et al., 2018a](#)). This has a great impact on the overall reactivity and the branching ratios of aromatic hydroxylated monocyclic compounds. Observations from the kinetic data of nitro containing aromatic hydrocarbons result in re-evaluation of the H-atom abstraction channel from the OH substituent, and a more suitable value for the reactions occurring at 298K is $k_{\text{abs}}(\text{Ph-OH}) = 1.4 \times 10^{-13}$ cm³ \times s⁻¹. EPI Suite – AOPWIN software 4.11 was developed based on [Kwok and Atkinson \(1995\)](#) observations by United States Environmental Protection Agency (US-EPA). Data in Table 4 shows that each SAR tends to overestimate the OH gas phase reactivity of hydroxylated nitrobenzenes. Along with nitrocatechols rate coefficient values obtained in the present study, Table 4 lists also the experimental kinetic rate coefficients for 2-nitrophenols determined by [Bejan et al. \(2007\)](#) and the estimated SAR

values. The 2-nitrophenols estimated rate coefficient values of [Jenkin et al. \(2018b\)](#) fit better with the experimental data compared with other SARs, due to the use of substituent adjustment factors $R(\Phi)$ for the substituent factors $F(\Phi)$ updated to the available literature and the rescaled of abstraction rate coefficient previously assigned to -OH groups in aliphatic compounds of $k_{\text{abs}}(\text{Ph-OH}) = 1.28 \times 10^{-12} \times \exp(-660/T) \text{ cm}^3 \times \text{ s}^{-1}$ ($1.4 \times 10^{-13} \text{ cm}^3 \times \text{ s}^{-1}$ at 298 K). In the case of nitrocatechols, [Jenkin et al. \(2018b\)](#) SAR values are a factor of 1.5 higher compared with the values of [Kwok and Atkinson \(1995\)](#). The difference between the estimated values is considered to appear due to the k_{add} estimation in [Kwok and Atkinson \(1995\)](#) SAR, where the electrophilic substituent coefficient τ^+ for the OH oriented in *-meta* position has no attributed contribution. For 1,2-dihydroxybenzenes molecules, the addition pathway might count only for one phenolic hydroxyl. This is in agreement with the experimental explanation given for 3-nitrocatechols reactivity, where the E^+ effect of the OH group from C2 has no electromeric effect on the aromatic ring as visible in infrared spectra. Consistency between the rate coefficient values is given as both SARs assume that the addition pathway is at least 94% of the overall reactivity. Based on the observations of [Bejan et al. \(2007\)](#) on methylated 2-nitrophenols, this assumption is reasonable.

As data in Table 4 show, no differences were observed between the rate coefficient values estimated by the EPI Suite – AOPWIN and [Kwok and Atkinson \(1995\)](#) approach since the programme is based on the model calculation proposed study. However, for nitrocatechols there is a difference between the rate coefficients values. This difference is observed since the programme could not choose the correct parameters of the nitro group to proper calculate $\Sigma\sigma^+$. Instead of choosing the lowest value for NO_2 substituent *-meta* orientated, it chooses the electrophilic substituent group constant from *-ortho* and *-para*, that gives the highest $\Sigma\sigma^+$, not the lowest as it is recommended. However, in further discussions we will no longer consider EPI Suite – AOPWIN software data.

In SAR approaches, the estimated rate coefficients values do not consider the interactions between the nitro and its vicinal OH group or between OH groups, thus all having a tendency to overestimate the gas phase OH rate coefficients for hydroxylated nitro monocyclic aromatics. However, [Jenkin et al. \(2018b\)](#) propose a substituent adjustment factor for NO_2 groups of 0.024 for the *-ortho* and *-para* relative to each of the addition sites on the ring and of 0.07 for the *-ipso* and *-meta* positions. In [Kwok and Atkinson \(1995\)](#), the SAR estimations assign the NO_2 group substituent factor of [Brown and Okamoto \(1958\)](#) of + 0.790 in *-ortho* or *-para* and of +0.674 for *-meta* or *-ipso*. All of these factors are calculated based on previous experimental data to fit alkyl substituted or low substituted aromatic compounds. Although the updated SAR of [Jenkin et al. \(2018b\)](#) is more complex, interactions between the substituents are not taken into consideration. These limitations lead in the case of 4NCAT or 4M5NCAT to different ratios of 5 and 18 times higher. For the 3NCAT and 5M3NCAT the estimated rate coefficient values are more consistent with the present experimental data, values being only ~2 times larger. Differences between experimental values of 4NCAT and 4M5NCAT in comparison with those estimated by SAR models suggest that the addition pathway is of lower importance compared with the H-atom abstraction from hydroxyl groups due to the inhibition of the E^+ effect of phenolic hydroxyls, and limited contribution from the presence of the CH_3 group.

355 If substituent interactions are taken into account by: (1) excluding the OH substituent effect on the addition channel (one substituent effect in 3NCAT, 5M3NCAT and both substituents in 4NCAT and 4M5NCAT); (2) removing one H-atom abstraction channel in all the nitrocatechols; (3) considering the methyl group inhibiting the H-atom abstraction channel in 4M5NCAT; and (4) using a new neighbouring group factor for α -H-atom abstraction from the deactivated phenolic group F(-Ph deactivated) = 0.5, then the automated mechanism construction proposed by [Jenkin et al. \(2018b\)](#) would emphasize
360 new estimated rate coefficient values approaching the experimental data obtained in this study as follows: for 3NCAT a rate of $3.95 \times 10^{-12} \text{ cm}^3 \times \text{s}^{-1}$ with a $k_{\text{add}}/k_{\text{tot}} = 0.67$, for 5M3NCAT a rate of $6.15 \times 10^{-12} \text{ cm}^3 \text{s}^{-1}$ with a $k_{\text{add}}/k_{\text{tot}} = 0.73$, for 4NCAT a rate of $2.36 \times 10^{-12} \text{ cm}^3 \times \text{s}^{-1}$ with a $k_{\text{add}}/k_{\text{tot}} = 0.45$ and for 4M5NCAT a rate of $3.71 \times 10^{-12} \text{ cm}^3 \times \text{s}^{-1}$ with a $k_{\text{add}}/k_{\text{tot}} = 0.69$.
365 However, based on the study of [Jenkin et al. \(2018b\)](#) and the behaviour of the investigated nitrocatechols it is probably better to use a value of 0.5 as a new parameter for the H-atom abstraction for the deactivated phenyl group F (-Ph deactivated) when $k_{\text{abs}}(\text{Ph-OH}) = 2.6 \times 10^{-12} \text{ cm}^3 \times \text{s}^{-1}$ is considered. In this case, the H-atom abstraction from phenolic hydroxyl will gain significant importance and will be in agreement with previous kinetic studies of hydroxylated aromatic compounds. The new estimated values obtained within the present work are listed in Table 4 besides those of methylated nitrophenols, for which systematic lower values are reported. Table TS2 from the supplementary material presents the revised estimated k_{OH} values for several nitroaromatic compounds using [Kwok and Atkinson \(1995\)](#) SAR model updated with recent observations.
370 Accounting for these experimental observations revisions for SAR model proposed by [Jenkin et al. \(2018b\)](#) were also performed. Figures 8 present the correlation analyses between the experimental, the original estimated and the revised estimated rate coefficients values. Thus, Figure 8A present such correlation *versus* the variation of the $\Sigma\sigma^+$ calculated without substituents interactions, while Figure 8B present this correlation *versus* the variation of the $\Sigma\sigma^+$ calculated when substituents interactions are taken into account. Data presented in both figures show that the main data cluster would be shifted to
375 positive $\Sigma\sigma^+$ when substituent interactions are considered in compliance with experimental values.

Figure 8C reflect the correlations between the estimated and experimental determined rate coefficient values for the interest nitrophenols and nitrocatechols. From Figure 8C it is evident that the estimated revised values show reduce outspread throughout correlation lines. Moreover, the correlation between estimated k_{OH} values derived from using group factors ([Jenkin et al. 2018](#)) *versus* estimated k_{OH} values derived using electrophilic substituents ([Kwok and Atkinson, 1995](#)) is
380 presented in Figure 8D. From the Figure 8D it is obvious that the original estimates values from both SAR methods present a poor correlation compare with the case when the same estimated k_{OH} values were generated after the revision based on the new obtained experimental data. The corrections introduced to account for the presence and influence of the H-bond to the rate coefficients values are reflected by the improvement in the Pearson coefficient value rising up from $r = 0.463$ for the original estimates to $r = 0.888$ for the revised estimates. However, the revised data seems to underestimate the experimental rate constant values for nitrophenols and overestimate those for nitrocatechols. Under these circumstances, it is strongly believed that new experimental values for the rate coefficients of nitroaromatics with OH radicals would further help to
385 better estimate the rate coefficient values for nitroaromatic compounds.

5.4. Atmospheric implications

The estimated photolysis frequencies for the 3NCAT and 5M3NCAT extrapolated to atmospheric conditions (see Table 2)
390 are comparable with those proposed by Bejan et al. (2007) for 2-nitrophenols. Photolysis of nitrocatechols with NO₂ and OH
groups in vicinal position would be the dominant atmospheric sink, being almost 10 times faster than reaction with OH
radicals. Similar values of photolysis frequencies have been also reported for nitro-naphthalenes and methyl-nitro-
naphthalenes (Phousongphouang and Arey, 2003). Based on the obtained data, it may be suggested that all the nitroaromatic
395 compounds that have the NO₂ group in vicinal position with a large electron density area, might easily undergo photolysis
which maybe is the main sink pathway in the atmosphere. Similar to 4-nitro and 5-nitrocatechols, dry or wet deposition
seems to be the most probable atmospheric removal process, with little or no photolysis in the boundary layer and with high
chemical residence time regarding atmospheric oxidative degradation initiated by OH radicals.

6. Conclusions

Gas-phase reaction rate coefficients of OH radicals with four nitrocatechols have been investigated for the first time by using
400 the ESC-Q-UAIC chamber facilities. The reactivity of all investigated nitrocatechols is strongly influenced by the formation
of intramolecular H-bonds that are directly influenced by the deactivating E-effect of the NO₂ group. For the 3-nitrocatechols
compounds, the electromeric effect of the "free" OH group is diminished by the deactivating E- effect of NO₂ group. Thus,
the rate coefficients of 3-nitrocatechols compounds are higher than the rate coefficients values of 4-nitrocatechol or 4-methyl-
5-nitrocatechol where no electromeric effect of the OH group seems to be active. In consequence, in 4-nitro or 5-
405 nitrocatechols the H-abstraction pathway seems to play an important role for the entire OH radical reaction while in 3-
nitrocatechols case the OH-addition path remains dominant.

For 3-nitrocatechols the atmospheric average lifetime seems to be controlled by the photolysis processes, similar to 2-
nitrophenols, with an average day-time lifetime of about one hour. Reaction with OH radicals is the main atmospheric
process for 4-nitrocatechols. Atmospheric day lifetimes of 4-nitro and 5-nitrocatechols are higher than 48 hours because of
410 the OH radical initiated oxidation, being susceptible to long-range transport at atmospheric conditions.

As presented in the current study, the automated mechanism construction for OH rate coefficients SAR estimations is further
recommended to consider the internal interactions between vicinal substituents. Moreover, all approaches tend to
overestimate the gas phase reactivity of highly substituted nitro containing aromatic compounds. Use of an average rate
coefficient for the H-atom abstraction from the O-H group $k_{\text{abs(Ph-OH)}} = 2.6 \times 10^{-12} \text{ cm}^3 \times \text{s}^{-1}$ is encouraged, along with a scaling
415 parameter for deactivated aromatic phenyl group, estimated to be 0.5 at 298 K. Also, the substituent adjustment factors R(Φ),
relative to the F(Φ) values for nitro group should be re-evaluated, R(Φ) average for all possible addition sites being ~ 0.009.
However, more studies are required to support the proposed reactivity for nitrocatechols and to move further the knowledge
of the gas-phase aromatic chemistry.

Competing interests

420 The authors declare no conflict of interest. The founders had no role in the design of the study; in the collection, analyses, or interpretation of data; in the writing of the manuscript, or in the decision to publish the results.

Author contribution

Claudiu ROMAN (Investigation, Formal analysis, Data curation, Writing – original draft, Writing – review & editing); Cecilia ARSENE (Data curation, Formal analysis, Funding acquisition, Writing – review & editing); Iustinian Gabriel 425 BEJAN (Formal analysis, Funding acquisition, Writing – review & editing); Romeo-Iulian OLARIU (Conceptualization, Formal analysis, Data curation, Funding acquisition, Supervision, Writing – review & editing).

Code availability

Not applicable

Acknowledgements

430 All authors acknowledge the financial support from European Union's Horizon 2020 - Research and Innovation Framework Programme, through the EUROCHAMP-2020 Infrastructure Activity Grant (grant agreement No 730997). C.R. and I.G.B. acknowledge the financial support offered by PN-III-P2-2.1-PED2019-4972 project from UEFISCDI. C.R. and R.I.O. are thankful to the support offer by UEFISCDI within the PN-III-P4-ID-PCE-2016-0270 Project (OLFA-ROA). Acknowledgment is given by C.A. and R.I.O. to infrastructure support from the Operational Program Competitiveness 435 2014–2020, Axis 1, under POC/448/1/1 Research infrastructure projects for public R&D institutions/Sections F 2018, through the Research Center with Integrated Techniques for Atmospheric Aerosol Investigation in Romania (RECENT AIR) project, under grant agreement MySMIS no. 127324.

References

Alif, A., Pilichowski, J. F. and Boule, P.: Photochemistry and environment XIII: Phototransformation of 2-nitrophenol in 440 aqueous solution, *J. Photochem. Photobiol. A Chem.*, 59(2), 209–219, doi:10.1016/1010-6030(91)87009-K, 1991.

Aschmann, S. M., Arey, J. and Atkinson, R.: Rate constants for the reactions of OH radicals with 1,2,4,5-tetramethylbenzene, pentamethylbenzene, 2,4,5-trimethylbenzaldehyde, 2,4,5-trimethylphenol, and 3-methyl-3-hexene-2,5-dione and products of OH + 1,2,4,5-tetramethylbenzene, *J. Phys. Chem.*, 117(12), 2556–2568, doi:10.1021/jp8074018, 2013.

Atkins, P. and de Paula, J.: *Physical Chemistry*, 8th Edit., Freeman, New York., 2006.

445 Atkinson, R.: Kinetics and mechanisms of the gas-phase reactions of the hydroxyl radical with organic compounds (Monograph 1), *J. Phys. Chem. Ref. Data*, 86(1), 1, doi:10.1021/cr00071a004, 1989.

Atkinson, R. and Aschmann, S. M.: Products of the gas-phase reactions of aromatic hydrocarbons: Effect of NO₂ concentration, *Int. J. Chem. Kinet.*, 26(9), 929–944, doi:10.1002/kin.550260907, 1994.

Atkinson, R., Aschmann, S. M., Arey, J., Barbara, Z. and Schuetzle, D.: Gas-phase atmospheric chemistry of 1- and 2-nitronaphthalene and 1,4-naphthoquinone, *Atmos. Environ.*, 23(12), 2679–2690, doi:10.1016/0004-6981(89)90548-9, 1989.

450 Atkinson, R., Aschmann, S. M. and Arey, J.: Reactions of hydroxyl and nitrogen trioxide radicals with phenol, cresols, and 2-nitrophenol at 296 ± 2K, *Environ. Sci. Technol.*, 26(7), 1397–1403, doi:10.1021/es00031a018, 1992.

Atkinson, R., Baulch, D. L., Cox, R. A., Crowley, J. N., Hampson, R. F., Hynes, R. G., Jenkin, M. E., Rossi, M. J. and Troe, J.: Evaluated kinetic and photochemical data for atmospheric chemistry: Part 1 - gas phase reactions of Ox, HOx, NOx and 455 SOx species, *Atmos. Chem. Phys.*, 4, 1461–1738, doi:10.5194/acpd-3-6179-2003, 2004.

Bejan, I., Abd El Aal, Y., Barnes, I., Benter, T., Bohn, B., Wiesen, P. and Kleffmann, J.: The photolysis of ortho-nitrophenols: a new gas phase source of HONO, *Phys. Chem. Chem. Phys.*, 8(17), 2028, doi:10.1039/b516590c, 2006.

Bejan, I., Barnes, I., Olariu, R., Zhou, S., Wiesen, P. and Benter, T.: Investigations on the gas-phase photolysis and OH radical kinetics of methyl-2-nitrophenols, *Phys. Chem. Chem. Phys.*, 9(42), 5686, doi:10.1039/b709464g, 2007.

460 Bejan, I., Schurmann, A., Barnes, I. and Benter, T.: Kinetics of the gas-phase reactions of OH radicals with a series of trimethylphenols, *Int. J. Chem. Kinet.*, 44(2), 117–124, doi:https://doi.org/10.1002/kin.20618, 2012.

Bejan, I., Olariu, R. and Wiesen, P.: Secondary organic aerosol formation from nitrophenols photolysis under atmospheric conditions, *Atmosphere (Basel.)*, 11(12), 1346, doi:10.3390/atmos11121346, 2020.

Bejan, I. G.: Investigations on the gas phase atmospheric chemistry of nitrophenols and catechols, Bergische Universität 465 Wuppertal. [online] Available from: <http://nbn-resolving.de/urn/resolver.pl?urn=urn%3Anbn%3Ade%3Ahbz%3A468-20070663>, 2006.

Belloli, R., Bolzacchini, E., Clerici, L., Rindone, B., Sesana, G. and Librando, V.: Nitrophenols in air and rainwater, *Environ. Eng. Sci.*, 23(2), 405–415, doi:10.1089/ees.2006.23.405, 2006.

Berndt, T. and Böge, O.: Gas-phase reaction of OH radicals with phenol, *Phys. Chem. Chem. Phys.*, 5(2), 342–350, 470 doi:10.1039/B208187C, 2003.

Bloss, C., Wagner, V., Jenkin, M. E., Volkamer, R., Bloss, W. J., Lee, J. D., Heard, D. E., Wirtz, K., Martin-Reviejo, M., Rea, G., Wenger, J. C. and Pilling, M. J.: Development of a detailed chemical mechanism (MCMv3.1) for the atmospheric oxidation of aromatic hydrocarbons, *Atmos. Chem. Phys.*, 5(3), 641–664, doi:10.5194/acp-5-641-2005, 2005.

Brown, H. and Okamoto, Y.: Electrophilic substituent constants, *J. Am. Chem. Soc.*, 80(18), 4979–4987, 1958.

475 Calvert, J. G., Atkinson, R., Becker, K. H., Kamens, R. M., Seinfeld, J. H., Wallington, T. J. and Yarwood, G.: The mechanisms of atmospheric oxidation of the aromatic hydrocarbons, Oxford University Press., 2002.

Coeur-Tourneur, C., Henry, F., Janquin, M. A. and Brutier, L.: Gas-phase reaction of hydroxyl radicals with m-, o- and p-cresol, *Int. J. Chem. Kinet.*, 38(9), 553–562, doi:10.1002/kin.20186, 2006.

480 Coeur-Tourneur, C., Foulon, V. and Laréal, M.: Determination of aerosol yields from 3-methylcatechol and 4-methylcatechol ozonolysis in a simulation chamber, *Atmos. Environ.*, 44(6), 852–857, doi:10.1016/j.atmosenv.2009.11.027, 2010a.

Coeur-Tourneur, C., Cassez, A. and Wenger, J. C.: Rate coefficients for the gas-phase reaction of hydroxyl radicals with 2-methoxyphenol (guaiacol) and related compounds, *J. Phys. Chem. A*, 114(43), 11645–11650, doi:10.1021/jp1071023, 2010b.

485 Delhomme, O., Morville, S. and Millet, M.: Seasonal and diurnal variations of atmospheric concentrations of phenols and nitrophenols measured in the Strasbourg area, France, *Atmos. Pollut. Res.*, 1(1), 16–22, doi:10.5094/APR.2010.003, 2010.

DeMore, W. B., Sander, S. P., Golden, D. M., Hampson, R. F., Kurylo, M. J., Howard, C. J., Ravishankara, A. R., Kolb, C. E. and Molina, M. J.: Chemical kinetics and photochemical data for use in stratospheric modeling., 1994.

Finewax, Z., De Gouw, J. A. and Ziemann, P. J.: Identification and quantification of 4-nitrocatechol formed from OH and 490 NO₃ radical-initiated reactions of catechol in air in the presence of NO_x: implications for secondary organic aerosol formation from biomass burning, *Environ. Sci. Technol.*, 52(4), 1981–1989, doi:10.1021/acs.est.7b05864, 2018.

Finlayson-Pitts, B. J. and Pitts, J. N.: Chemistry of the upper and lower atmosphere, Academic Press., 2000.

Grosjean, D.: Atmospheric fate of toxic aromatic compounds, *Sci. Total Environ.*, 100(C), 367–414, doi:10.1016/0048-9697(91)90386-S, 1991.

495 Harrison, M. A. J., Barra, S., Borghesi, D., Vione, D., Arsene, C. and Olariu, R. I.: Nitrated phenols in the atmosphere: A review, *Atmos. Environ.*, 39(2), 231–248, doi:10.1016/j.atmosenv.2004.09.044, 2005.

Herterich, R.: Gas chromatographic determination of nitrophenols in atmospheric liquid water and airborne particulates, *J. Chromatogr. A*, 549(C), 313–324, doi:10.1016/S0021-9673(00)91442-0, 1991.

Herterich, R. and Herrmann, R.: Comparing the distribution of nitrated phenols in the atmosphere of two german hill sites, 500 *Environ. Technol.*, 11(10), 961–972, doi:10.1080/09593339009384948, 1990.

Hine, J. and Mookerjee, P. K.: The intrinsic hydrophilic character of organic compounds. Correlations in terms of structural contributions, *J. Org. Chem.*, 40(3), 292–298, doi:10.1021/jo00891a006, 1975.

Hofzumahaus, A., Kraus, A. and Müller, M.: Solar actinic flux spectroradiometry: a technique for measuring photolysis frequencies in the atmosphere, *Appl. Opt.*, 38(21), 4443, doi:10.1364/ao.38.004443, 1999.

505 Iinuma, Y., Böge, O. and Herrmann, H.: Methyl-nitrocatechols: Atmospheric tracer compounds for biomass burning secondary organic aerosols, *Environ. Sci. Technol.*, 44(22), 8453–8459, doi:10.1021/es102938a, 2010.

Ikemori, F., Nakayama, T. and Hasegawa, H.: Characterization and possible sources of nitrated mono- and di-aromatic hydrocarbons containing hydroxyl and/or carboxyl functional groups in ambient particles in Nagoya, Japan, *Atmos. Environ.*, 211, 91–102, doi:10.1016/j.atmosenv.2019.05.009, 2019.

510 Jenkin, M. E., Derwent, R. G. and Wallington, T. J.: Photochemical ozone creation potentials for volatile organic compounds: Rationalization and estimation, *Atmos. Environ.*, 163, 128–137, doi:10.1016/j.atmosenv.2017.05.024, 2017.

Jenkin, M. E., Valorso, R., Aumont, B., Rickard, A. R. and Wallington, T. J.: Estimation of rate coefficients and branching

ratios for gas-phase reactions of OH with aliphatic organic compounds for use in automated mechanism construction, *Atmos. Chem. Phys.*, 18(13), 9297–9328, doi:10.5194/acp-18-9297-2018, 2018a.

515 Jenkin, M. E., Valorso, R., Aumont, B., Rickard, A. R. and Wallington, T. J.: Estimation of rate coefficients and branching ratios for gas-phase reactions of OH with aromatic organic compounds for use in automated mechanism construction, *Atmos. Chem. Phys.*, 18(13), 9329–9349, doi:10.5194/acp-18-9329-2018, 2018b.

Kitanovski, Z., Grgić, I., Yasmine, F., Claeys, M. and Čusak, A.: Development of a liquid chromatographic method based on ultraviolet-visible and electrospray ionization mass spectrometric detection for the identification of nitrocatechols and 520 related tracers in biomass burning atmospheric organic aerosol, *Rapid Commun. Mass Spectrom.*, 26(7), 793–804, doi:10.1002/rcm.6170, 2012a.

Kitanovski, Z., Grgić, I., Vermeylen, R., Claeys, M. and Maenhaut, W.: Liquid chromatography tandem mass spectrometry method for characterization of monoaromatic nitro-compounds in atmospheric particulate matter, *J. Chromatogr. A*, 1268, 35–43, doi:10.1016/j.chroma.2012.10.021, 2012b.

525 Kitanovski, Z., Hovorka, J., Kuta, J., Leoni, C., Prokeš, R., Sáňka, O., Shahpoury, P. and Lammel, G.: Nitrated monoaromatic hydrocarbons (nitrophenols, nitrocatechols, nitrosalicylic acids) in ambient air: levels, mass size distributions and inhalation bioaccessibility, *Environ. Sci. Pollut. Res.*, doi:10.1007/s11356-020-09540-3, 2020.

Klotz, B., Barnes, I., Becker, K. H. and Golding, B. T.: Atmospheric chemistry of benzene oxide/oxepin, *J. Chem. Soc. - Faraday Trans.*, 93(8), 1507–1516, doi:10.1039/a606152d, 1997.

530 Klotz, B., Sørensen, S., Barnes, I., Becker, K. H., Etzkorn, T., Volkamer, R., Platt, U., Wirtz, K. and Martin-Reviejo, M.: Atmospheric oxidation of toluene in a large-volume outdoor photoreactor: In situ determination of ring-retaining product yields, *J. Phys. Chem. A*, 102, 10289–10299, doi:10.1021/jp982719n, 1998.

Klotz, B., Volkamer, R., Hurley, M. D., Andersen, M. P. S., Nielsen, O. J., Barnes, I., Imamura, T., Wirtz, K., Becker, K. H., Platt, U., Wallington, T. J. and Washida, N.: OH-initiated oxidation of benzene part II. Influence of elevated NO_x 535 concentrations, *Phys. Chem. Chem. Phys.*, 4(18), 4399–4411, doi:10.1039/b204398j, 2002.

Kwok, E. and Atkinson, R.: Estimation of hydroxyl radical reaction rate constants for gas-phase organic compounds using a structure-reactivity relationship: An update, *Atmos. Environ.*, 29(14), 1685–1695, doi:10.1016/1352-2310(95)00069-B, 1995.

Lanzafame, G. M., Srivastava, D., Favez, O., Bandowe, B. A. M., Shahpoury, P., Lammel, G., Bonnaire, N., Alleman, L. Y., 540 Couvidat, F., Bessagnet, B. and Albinet, A.: One-year measurements of secondary organic aerosol (SOA) markers in the Paris region (France): Concentrations, gas/particle partitioning and SOA source apportionment, *Sci. Total Environ.*, 757, 143921, doi:10.1016/j.scitotenv.2020.143921, 2021.

Lauraguais, A., Coeur-Tourneur, C., Cassez, A., Deboudt, K., Fourmentin, M. and Choël, M.: Atmospheric reactivity of hydroxyl radicals with guaiacol (2-methoxyphenol), a biomass burning emitted compound: Secondary organic aerosol 545 formation and gas-phase oxidation products, *Atmos. Environ.*, 86, doi:10.1016/j.atmosenv.2013.11.074, 2014.

Lauraguais, A., Bejan, I., Barnes, I., Wiesen, P. and Coeur, C.: Rate coefficients for the gas-phase reactions of hydroxyl

radicals with a series of methoxylated aromatic compounds, *J. Phys. Chem. A*, 119(24), 6179–6187, doi:10.1021/acs.jpca.5b03232, 2015.

Leuenberger, C., Czuczwa, J., Heyerdahl, E. and Giger, W.: Aliphatic and polycyclic aromatic hydrocarbons in urban rain, snow and fog, *Atmos. Environ.*, 22(4), 695–705, doi:10.1016/0004-6981(88)90007-8, 1988.

550 Lin, P., Aiona, P. K., Li, Y., Shiraiwa, M., Laskin, J., Nizkorodov, S. A. and Laskin, A.: Molecular characterization of brown carbon in biomass burning aerosol particles, *Environ. Sci. Technol.*, 50(21), 11815–11824, doi:10.1021/acs.est.6b03024, 2016.

Lüttke, J., Scheer, V., Levsen, K., Wünsch, G., Cape, J. N., Hargreaves, K. J., Storeton-West, R. L., Acker, K., Wieprecht, W. and Jones, B.: Occurrence and formation of nitrated phenols in and out of cloud, *Atmos. Environ.*, 31(16), 2637–2648, doi:10.1016/S1352-2310(96)00229-4, 1997.

555 Meylan, W. M. and Howard, P. H.: Bond contribution method for estimating Henry's law constants, *Environ. Toxicol. Chem.*, 10, 1283, doi:10.1897/1552-8618(1991)10[1283:bcmfeh]2.0.co;2, 1991.

Olariu, R. I., Barnes, I., Becker, K. H. and Klotz, B.: Rate coefficients for the gas-phase reaction of OH radicals with 560 selected dihydroxybenzenes and benzoquinones, *Int. J. Chem. Kinet.*, 32(11), 696–702, 2000.

Olariu, R. I., Klotz, B., Barnes, I., Becker, K. H. and Mocanu, R.: FT-IR study of the ring-retaining products from the reaction of OH radicals with phenol, o-, m-, and p-cresol, *Atmos. Environ.*, 36(22), 3685–3697, doi:10.1016/S1352-2310(02)00202-9, 2002.

565 Olariu, R. I., Bejan, I., Barnes, I., Klotz, B., Becker, K. H. and Wirtz, K.: Rate coefficients for the gas-phase reaction of NO_3 radicals with selected dihydroxybenzenes, *Int. J. Chem. Kinet.*, 36(11), 577–583, doi:10.1002/kin.20029, 2004.

Olariu, R. I., Barnes, I., Bejan, I., Arsene, C., Vione, D., Klotz, B. and Becker, K. H.: FT-IR product study of the reactions of NO_3 radicals with ortho -, meta -, and para-cresol, *Environ. Sci. Technol.*, 47(14), 7729–7738, doi:10.1021/es401096w, 2013.

570 Palumbo, A., Napolitano, A. and D'Ischia, M.: Nitrocatechols versus nitrocatecholamines as novel competitive inhibitors of neuronal nitric oxide synthase: Lack of the aminoethyl side chain determines loss of tetrahydrobiopterin-antagonizing properties, *Bioorganic Med. Chem. Lett.*, 12(1), 13–16, doi:10.1016/S0960-894X(01)00680-1, 2002.

Phousongphouang, P. T. and Arey, J.: Rate constants for the photolysis of the nitronaphthalenes and methylnitronaphthalenes, *J. Photochem. Photobiol. A Chem.*, 157(2–3), 301–309, doi:10.1016/S1010-6030(03)00072-8, 2003.

575 Piccot, S. D., Watson, J. J. and Jones, J. W.: A global inventory of volatile organic compound emissions from anthropogenic sources, *J. Geophys. Res.*, 97(D9), 9897–9912, doi:10.1029/92JD00682, 1992.

Prinn, R. G., Weiss, R. F., Miller, B. R., Huang, J., Alyea, F. N., Cunnold, D. M., Fraser, P. J., Hartley, D. E. and Simmonds, P. G.: Atmospheric trends and lifetime of CH_3CCl_3 and global OH concentrations, *Science* (80- .), 269(5221), 187–192, doi:10.1126/science.269.5221.187, 1995.

580 Richartz, H., Reischl, A., Trautner, F. and Hutzinger, O.: Nitrated phenols in fog, *Atmos. Environ. Part A, Gen. Top.*,

24(12), 3067–3071, doi:10.1016/0960-1686(90)90485-6, 1990.

Roman, C., Roman, T., Arsene, C., Bejan, I. G. and Olariu, R. I.: Gas-phase IR cross-sections and single crystal structures data for atmospheric relevant nitrocatechols, *Spectrochim. Acta - Part A Mol. Biomol. Spectrosc.*, 265(x), 120379, doi:10.1016/j.saa.2021.120379, 2022.

585 Rosenblatt, D. H., Epstein, T. and Levitch, M.: Some nuclearly substituted catechols and their acid dissociation constants, *J. Am. Chem. Soc.*, 75(13), 3277–3278, doi:10.1021/ja01109a511, 1953.

Rubio, M. A., Lissi, E., Herrera, N., Pérez, V. and Fuentes, N.: Phenol and nitrophenols in the air and dew waters of Santiago de Chile, *Chemosphere*, 86(10), 1035–1039, doi:10.1016/j.chemosphere.2011.11.046, 2012.

590 Salvador, C. M. G., Tang, R., Priestley, M., Li, L., Tsiligiannis, E., Le Breton, M., Zhu, W., Zeng, L., Wang, H., Yu, Y., Hu, M., Guo, S. and Hallquist, M.: Ambient nitro-aromatic compounds-biomass burning versus secondary formation in rural China, *Atmos. Chem. Phys.*, 21(3), 1389–1406, doi:10.5194/acp-21-1389-2021, 2021.

Schauer, J. J., Kleeman, M. J., Cass, G. R. and Simoneit, B. R. T.: Measurement of emissions from air pollution sources. 3. C1-C29 organic compounds from fireplace combustion of wood, *Environ. Sci. Technol.*, 35(9), 1716–1728, doi:10.1021/es001331e, 2001.

595 Schwantes, R. H., Schilling, K. A., McVay, R. C., Lignell, H., Coggon, M. M., Zhang, X., Wennberg, P. O. and Seinfeld, J. H.: Formation of highly oxygenated low-volatility products from cresol oxidation, *Atmos. Chem. Phys.*, 17(5), 3453–3474, doi:10.5194/acp-17-3453-2017, 2017.

600 Sørensen, M., Hurley, M. D., Wallington, T. J., Dibble, T. S. and Nielsen, O. J.: Do aerosols act as catalysts in the OH radical initiated atmospheric oxidation of volatile organic compounds?, *Atmos. Environ.*, 36(39–40), 5947–5952, doi:10.1016/S1352-2310(02)00766-5, 2002.

Taylor, W. D., Allston, T. D., Moscato, M. J., Fazekas, G. B., Kozlowski, R. and Takacs, G. A.: Atmospheric photodissociation lifetimes for nitromethane, methyl nitrite, and methyl nitrate, *Int. J. Chem. Kinet.*, 12(4), 231–240, doi:10.1002/kin.550120404, 1980.

605 Thüner, L. P., Bardini, P., Rea, G. J. and Wenger, J. C.: Kinetics of the gas-phase reactions of OH and NO₃ radicals with dimethylphenols, *J. Photochem. Photobiol. A Chem.*, 108(), 11019–11025, doi:10.1021/jp046358p, 2004.

Vanni, A., Pellegrino, V., Gamberini, R. and Calabria, A.: An evidence for nitrophenols contamination in antarctic freshwater and snow. Simultaneous determination of nitrophenols and nitroarenes at ng/L levels, *Int. J. Environ. Anal. Chem.*, 79(4), 349–365, doi:10.1080/03067310108044394, 2001.

610 Vidović, K., Lašić Jurković, D., Šala, M., Kroflič, A. and Grgić, I.: Nighttime aqueous-phase formation of nitrocatechols in the atmospheric condensed phase, *Environ. Sci. Technol.*, 52(17), 9722–9730, doi:10.1021/acs.est.8b01161, 2018.

Volkamer, R., Klotz, B., Barnes, I., Imamura, T., Wirtz, K., Washida, N., Becker, K. H. and Platt, U.: OH-initiated oxidation of benzene, *Phys. Chem. Chem. Phys.*, 4(9), 1598–1610, doi:10.1039/b108747a, 2002.

Vozňáková, Z., Podehradská, J. and Kohlíčková, M.: Determination of nitrophenols in soil, *Chemosphere*, 33(2), 285–291, doi:10.1016/0045-6535(96)00171-3, 1996.

615 Wang, Z., Zhang, J., Zhang, L., Liang, Y. and Shi, Q.: Characterization of nitroaromatic compounds in atmospheric particulate matter from Beijing, *Atmos. Environ.*, 246(May 2020), 118046, doi:10.1016/j.atmosenv.2020.118046, 2021.

Warneck, P.: *Chemistry of the Natural Atmosphere*, Second Edi., edited by P. Warneck, Academic Press., 2000.

Wilson, E. W., Hamilton, W. A., Kennington, H. R., Evans, B., Scott, N. W. and Demore, W. B.: Measurement and estimation of rate constants for the reactions of hydroxyl radical with several alkanes and cycloalkanes, *J. Phys. Chem. A*, 620 110(10), 3593–3604, doi:10.1021/jp055841c, 2006.

Witte, F., Urbanik, E. and Zetzs, C.: Temperature dependence of the rate constants for the addition of OH to benzene and to some monosubstituted aromatics (aniline, bromobenzene, and nitrobenzene) and the unimolecular decay of the adducts. Kinetics into a quasi-equilibrium, *J. Phys. Chem.*, 90(14), 3251–3259, doi:10.1021/j100405a040, 1986.

Zetzs, C.: Predicting the rate of OH-addition to aromatics using $\sigma+$ -electrophilic substituents constants for mono- and 625 polysubstituted benzene, in *XIth Informal Conference on Photochemistry*, Stanford, California, 27. 6. - 1. 7, Stanford Res. Inst., California., 1982.

Zhang, Y., Forrister, H., Liu, J., Dibb, J., Anderson, B., Schwarz, J. P., Perring, A. E., Jimenez, J. L., Campuzano-Jost, P., Wang, Y., Nenes, A. and Weber, R. J.: Top-of-atmosphere radiative forcing affected by brown carbon in the upper troposphere, *Nat. Geosci.*, 10(7), 486–489, doi:10.1038/ngeo2960, 2017.

630

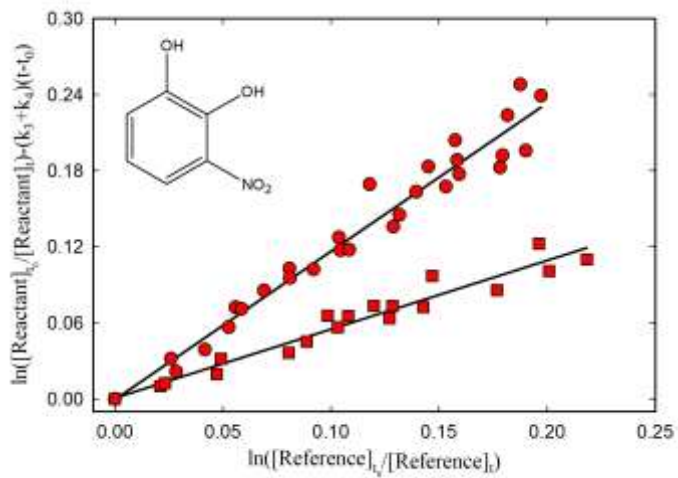
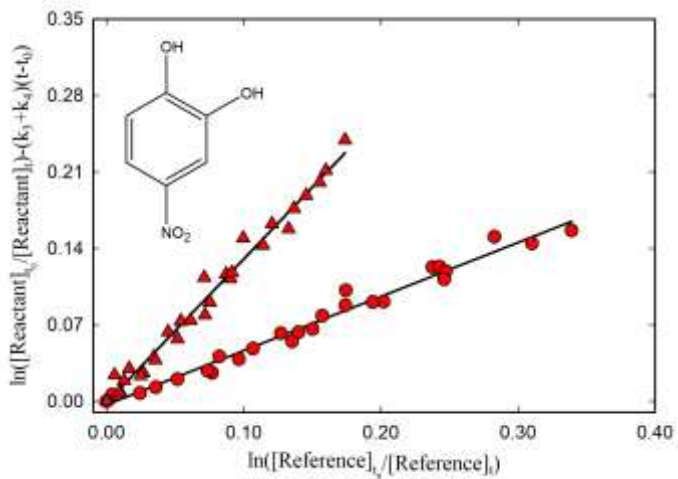


Figure 1: Kinetic plot according to Eq. 1 for the reaction of 3-nitrocatechol with OH radicals relative to (●) dimethyl ether and (■) cyclohexane, using photolysis of $\text{CH}_3\text{ONO}/\text{NO}$ mixture at 365 nm as OH radical source.



635

Figure 2: Kinetic plot according to Eq. 1 for the reaction of 4-nitrocatechol with OH radicals relative to (●) dimethyl ether, using photolysis of $\text{CH}_3\text{ONO}/\text{NO}$ mixture at 365 nm as OH-radical source, and relative to (▲) methanol, using photolysis of H_2O_2 at 254 nm as OH-radical source.

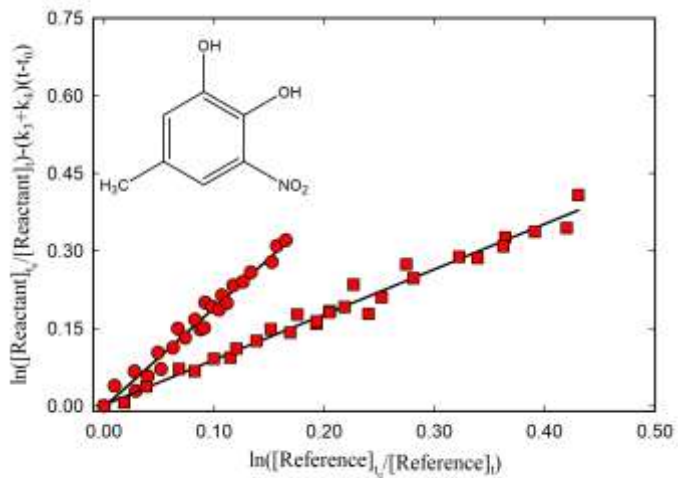
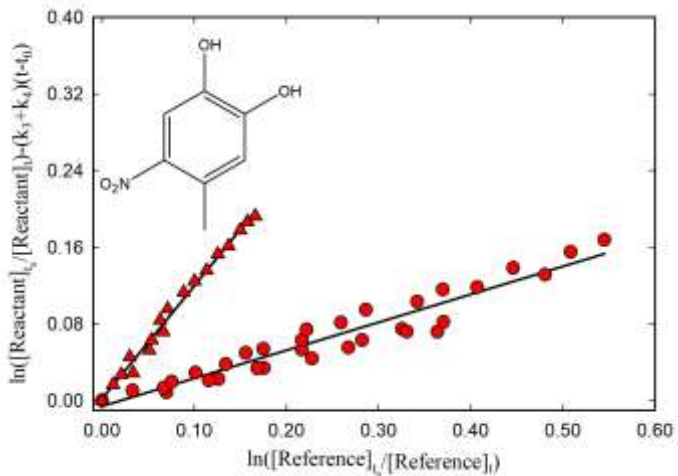


Figure 3: Kinetic plot according to Eq. 1 for the reaction of 5-methyl-3-nitrocatechol with OH radicals relative to (●) dimethyl ether and (■) cyclohexane using photolysis of $\text{CH}_3\text{ONO}/\text{NO}$ mixture at 365 nm as OH radical source.



645 **Figure 4:** Kinetic plot according to Eq. 1 for the reaction of 4-methyl-5-nitrocatechol with OH radicals relative to (●) dimethyl ether, using photolysis of $\text{CH}_3\text{ONO}/\text{NO}$ mixture at 365 nm as OH-radical source, and relative to (▲) methanol, using photolysis of H_2O_2 at 254 nm as OH-radical source.

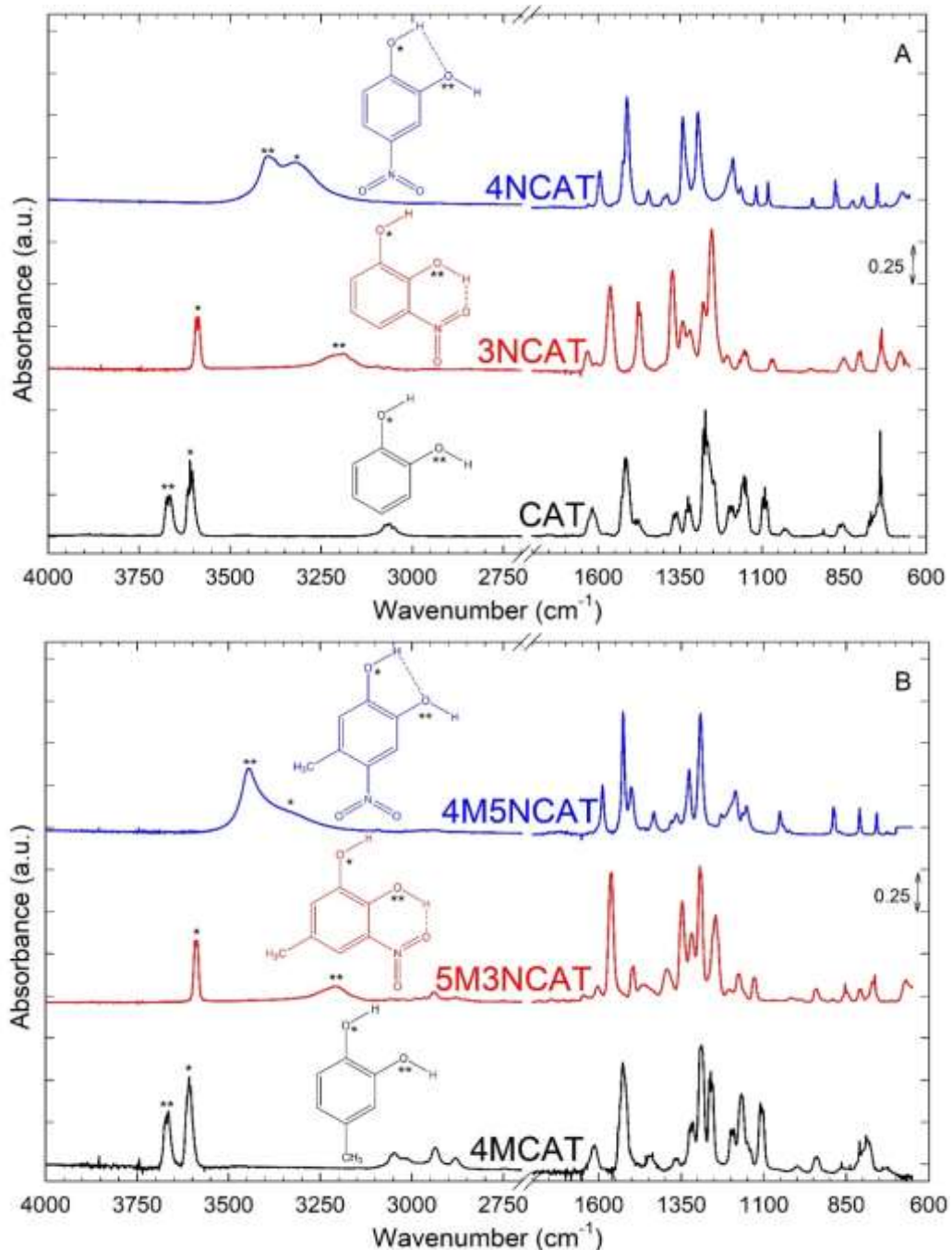
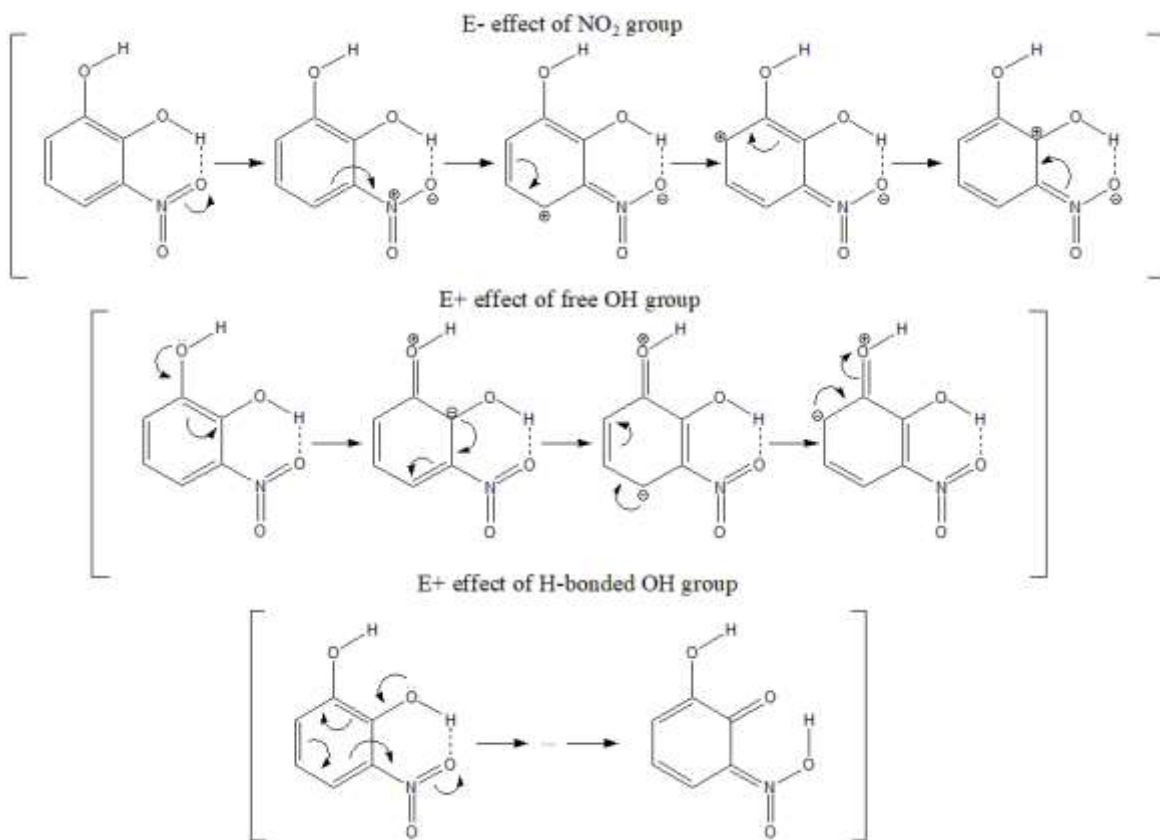


Figure 5: A - Gas-phase IR spectra of catechol (CAT), **3NCAT**, **4NCAT**;

B - Gas-phase IR spectra of 4-methylcatechol (4MCAT), **5M3NCAT** and **4M5NCAT**.

Evidence for the intramolecular H-bond occurrence between the substituents marked with */**: catechol and 4MCAT – both free OH present in the spectra; **3NCAT** and **5M3NCAT** – only one free OH; **4NCAT** and **4M5NCAT** – both OH involved in H-bond.



660 **Figure 6:** Electromeric effects of NO_2 and OH substituents from 3NCAT molecule.

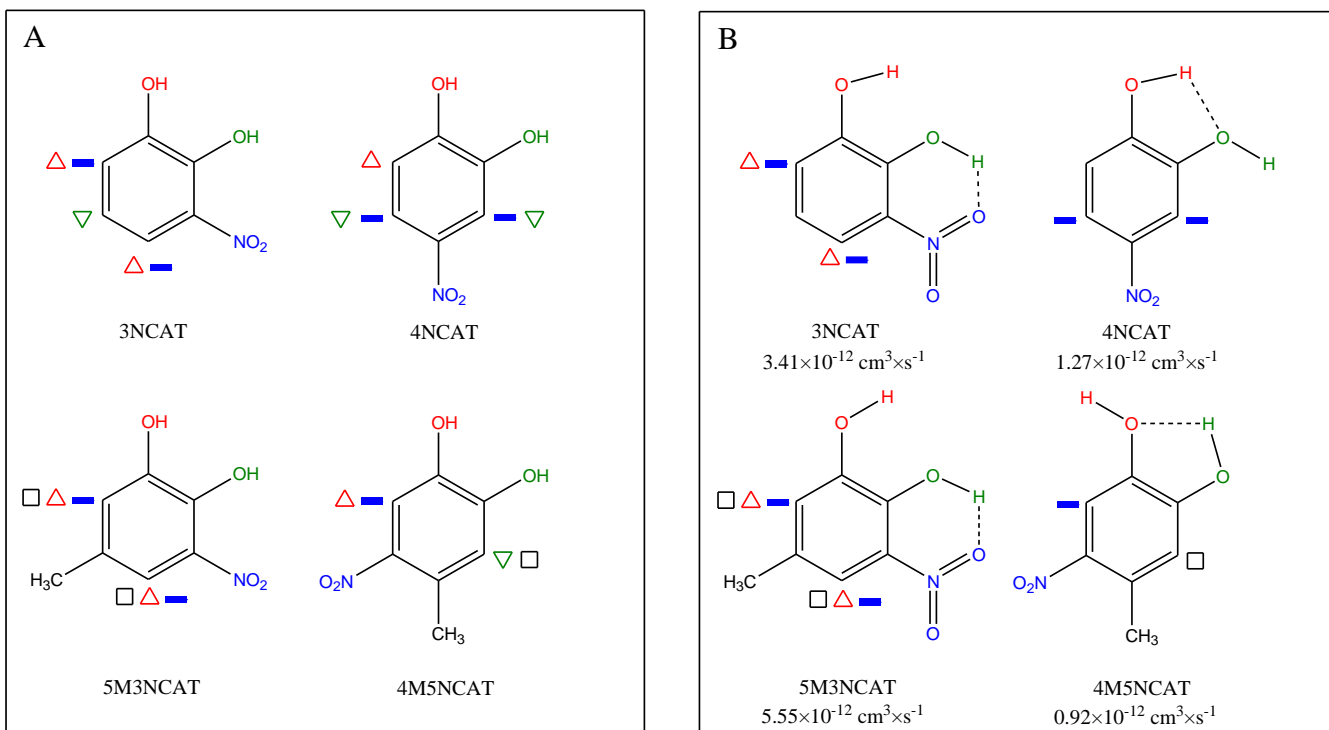
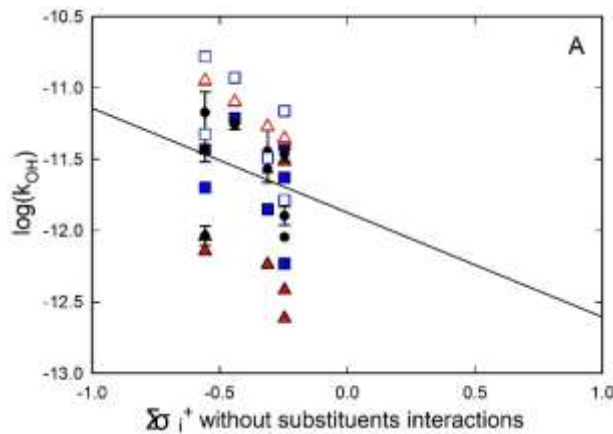
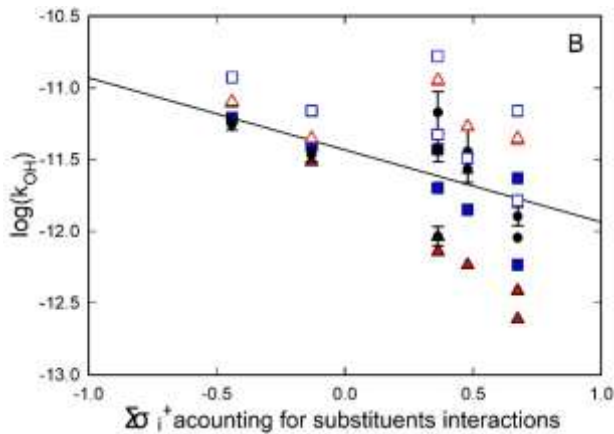


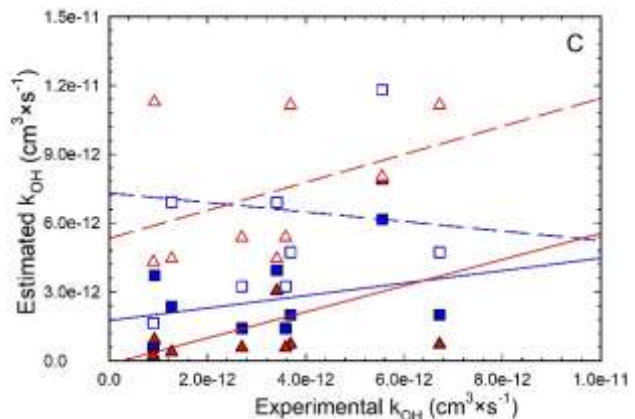
Figure 7: Electromeric effect distribution on the aromatic ring for the all investigating nitrocatechols in the present study: (A) active sites toward electrophilic attack by hydroxyl (1st OH Δ / 2nd OH ∇), nitro (—) and methyl (□) groups; (B) internal interactions of the substituents and consequences on the reactivity based on the gas phase FT-IR spectra.



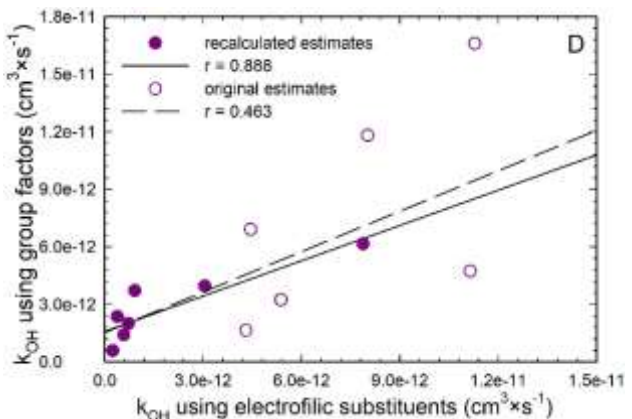
Legend 8A: (●) k_{OH} experimental data of nitrophenols and nitrocatechols; (■) revised data of SAR estimates from Jenkin et al. (2018b) (see text); (▲) revised data of SAR estimates from Kwok and Atkinson (1995) (see text); (□) original SAR estimates data from Jenkin et al. (2018b); (△) original SAR estimates data from Kwok and Atkinson (1995);



Legend 8B: (●) k_{OH} experimental data of nitrophenols and nitrocatechols; (■) revised data of SAR estimates from Jenkin et al. (2018b) (see text); (▲) revised data of SAR estimates from Kwok and Atkinson (1995) (see text); (□) original SAR estimates data from Jenkin et al. (2018b); (△) original SAR estimates data from Kwok and Atkinson (1995);



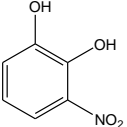
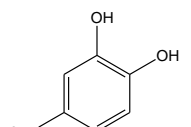
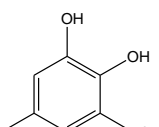
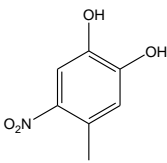
Legend 8C: (■) revised data of SAR estimates from Jenkin et al. (2018b) (see text); (▲) revised data of SAR estimates from Kwok and Atkinson (1995) (see text); (□) original SAR estimates data from Jenkin et al. (2018b); (△) original SAR estimates data from Kwok and Atkinson (1995).



Legend 8D: (●) re-evaluated data; (○) original data.

Figure 8: Correlation analyses between the experimental, the original estimated and the revised estimated rate coefficients values.

Table 1: Rate coefficient values of OH radical reactions with all investigated nitrocatechols in the present study.

Compound	Referent	k_1/k_2	k_1 [$10^{-12} \text{ cm}^3 \times \text{s}^{-1}$]	k_1 (average) [$10^{-12} \text{ cm}^3 \times \text{s}^{-1}$]	τ^a [h]
 3-nitrocatechol	DME	1.17 ± 0.09	3.27 ± 0.69	3.41 ± 0.37	51.6
	Cyclohexane	0.54 ± 0.06	3.46 ± 0.44		
 4-nitrocatechol	DME	0.49 ± 0.03	1.39 ± 0.29	1.27 ± 0.19	137.0
	Methanol	1.31 ± 0.06	1.18 ± 0.24		
 5-methyl-3-nitrocatechol	DME	1.92 ± 0.13	5.37 ± 1.14	5.55 ± 0.48	31.3
	Cyclohexane	0.88 ± 0.05	5.58 ± 0.49		
 4-methyl-5-nitrocatechol	DME	0.29 ± 0.03	0.82 ± 0.18	0.92 ± 0.14	189.6
	Methanol	1.18 ± 0.06	1.06 ± 0.22		

^a calculated considering the average daytime OH radical concentration of $1.6 \times 10^6 \text{ cm}^{-3}$ (Prinn et al., 1995).

Table 2: Rate coefficients values for the photolysis of all nitrocatechols investigated in this study scaled to atmospheric conditions and their average atmospheric lifetimes due to the photolysis (at 365 nm).

Compound	$J_{(\text{NCAT}) - 254 \text{ nm}}$ [10^{-4} s^{-1}]	$J_{(\text{NCAT}) - 365 \text{ nm}}$ [10^{-4} s^{-1}]	τ_{hv} (at 365 nm) [h]
3NCAT	not measured	3.06 ± 0.16	~ 0.91
4NCAT	0.67 ± 0.01	< 0.1	> 27.78
5M3NCAT	not measured	2.14 ± 0.18	~ 1.30
4M5NCAT	0.32 ± 0.03	< 0.1	> 27.78

Table 3: Rate coefficients at 298 K for aromatic hydrocarbons (AHs) and their correspondent nitroaromatic (NAHs) derivates for the gas-phase reaction with the OH radical.

Aromatic hydrocarbon (AHs)	k_{OH} [$10^{-12} \text{ cm}^3 \times \text{s}^{-1}$]	Nitroaromatic hydrocarbon (NAHs)	k_{OH} [$10^{-12} \text{ cm}^3 \times \text{s}^{-1}$]	$k_{\text{NAHs}}/k_{\text{AHs}}$ (%)
benzene	1.22 ^a	nitrobenzene	0.14 ^{a,b}	11.48
toluene	5.63 ^a	<i>m</i> -nitrotoluene	1.20 ^a	21.31
phenol	26.3 ^{a,d}	2-nitrophenol	0.90 ^c	3.42
<i>o</i> -cresol	41 ^{a,d}	6-methyl-2-nitrophenol	2.70 ^e	6.59
<i>m</i> -cresol	68 ^{a,d}	3-methyl-2-nitrophenol	3.69 ^e	5.43
		5-methyl-2-nitrophenol	6.72 ^e	9.88
<i>p</i> -cresol	50 ^{a,c}	4-methyl-2-nitrophenol	3.59 ^e	7.18
catechol	104 ^f	3-nitrocatechol	3.41 ^g	3.28
		4-nitrocatechol	1.27 ^g	1.22
4-methylcatechol	156 ^f	5-methyl-3-nitrocatechol	5.55 ^g	3.56
		4-methyl-5-nitrocatechol	0.92 ^g	0.59
naphthalene	23.00 ^a	1-nitronaphthalene	5.40 ^h	23.48
		2-nitronaphthalene	5.60 ^h	24.35

^aCalvert et al. (2002); ^bWitte et al., (1986), ^cAtkinson et al. (1992); ^dAtkinson (1989); ^eBejan et al. (2007); ^fOlariu et al. (2000); ^gThis work, ^h(Atkinson et al., 1989).

685 **Table 4:** Experimental and SAR-estimated rate coefficients of monoaromatic hydroxylated nitro compounds with the
radicals. In brackets are the ratios of the estimated values versus experimental data ($k_{\text{calc}}/k_{\text{exp}}$).

Compound	Experimental data	EPI Suite - AOPWIN	Kwok and Atkinson 1995	SAR		
				<i>Jenkin et al., 2018b</i>		this work
				$k_{\text{abs}}(\text{Ph-OH})$	2.6×10^{-12}	
				$k_{(\text{OH})} \times 10^{12}$ [cm ³ × s ⁻¹]		
3NCAT	3.41 ± 0.37	3.15 (0.92)	4.45 (1.30)	11.83 (3.47)	6.91 (2.03)	3.95 (1.16)
4NCAT	1.27 ± 0.19	3.15 (2.48)	4.45 (3.50)	11.83 (9.31)	6.91 (5.44)	2.36 (1.86)
5M3NCAT	5.55 ± 0.48	5.65 (1.02)	8.02 (1.45)	18.21 (3.28)	11.81 (2.13)	6.15 (1.11)
4M5NCAT	0.92 ± 0.14	7.90 (8.59)	11.29 (12.27)	22.99 (25.00)	16.60 (18.04)	3.71 (4.03)
3M2NPh	$3.69 \pm 0.70^{\text{a}}$	11.15 (3.02)	11.15 (3.02)	7.19 (1.95)	4.73 (1.28)	2.00 (0.54)
4M2NPh	$3.59 \pm 1.17^{\text{a}}$	5.38 (1.50)	5.38 (1.50)	7.17 (2.00)	3.24 (0.90)	1.41 (0.39)
5M2NPh	$6.72 \pm 2.14^{\text{a}}$	11.15 (1.66)	11.15 (1.66)	7.19 (1.07)	4.73 (0.70)	2.00 (0.30)
6M2NPh	$2.70 \pm 0.57^{\text{a}}$	5.38 (1.99)	5.38 (1.99)	7.17 (2.66)	3.24 (1.20)	1.41 (0.52)

^aValues from Bejan et al. (2007): 3M2NPh- 3-methyl-2-nitrophenol; 4M2NPh- 4-methyl-2-nitrophenol; 5M2NPh- 5-methyl-2-nitrophenol; 6M2NPh- 6-methyl-2-nitrophenol.